Vol. 625: 225–231, 2019
https://doi.org/10.3354/meps13079

MARINE ECOLOGY PROGRESS SERIES
Mar Ecol Prog Ser

Published August 29

NOTE

Herding mesopelagic fish by light

Stein Kaartvedt[1,*], Anders Røstad[2], Anders Frugård Opdal[3], Dag L. Aksnes[3]

[1]Department of Biosciences, University of Oslo, PO Box 1066, Blindern, 0316 Oslo, Norway
[2]Red Sea Research Center, King Abdullah University of Science and Technology, Thuwal 23955-6900, Saudi Arabia
[3]Department of Biological Sciences, University of Bergen, Bergen 5020, Norway

ABSTRACT: To assess organisms forming mesopelagic scattering layers in the Red Sea, we took advantage of their reactions to light. We used a remotely operated vehicle (ROV) equipped with LED lamps for herding the acoustic targets down to the bottom (700 m), while concurrently monitoring the event by shipborne and deployed echosounders as well as video footage from the ROV. In essence, entire mesopelagic scattering layers at 38 kHz were moved downwards until the organisms became trapped and concentrated at the bottom and identified as fish from video images. However, responses to the artificial light source appeared to include both repulsion and attraction. An individual-based model reproduced the herding event by assuming a dichotomous response to light where targets close to the light source are attracted, while targets further away are repulsed. We hypothesize that attraction is associated with the artificial light acting as a point source (beam light), while the repulsion is associated with the artificial light acting as diffuse light.

KEY WORDS: Artificial light · Repulsion · Attraction · Echosounder · Video · Individual-based model

1. INTRODUCTION

Mesopelagic sound scattering layers (SSL) occur worldwide (Bianchi et al. 2013, Irigoien et al. 2014). The organisms forming the SSL to a varying extent carry out diel vertical migration (DVM), apparently playing a significant role in the biological pump (Bianchi et al. 2013, Davison et al. 2013, Klevjer et al. 2016) as well as in marine food webs in general (Irigoien et al. 2014). Light appears to be a first-order driver for observed daytime distributions and DVM patterns in all ocean regions (reviewed in Kaartvedt et al. 2019). Several SSL studies suggest that the acoustic targets tend to stay within certain light levels, typically spanning some orders of magnitude (Kampa 1971, Aksnes et al. 2017). At mesopelagic depths during daytime the sunlight is diffuse, i.e. the sun is not perceived as a point source. It appears that the twilight organisms avoid diffuse light that is too strong, explaining why mesopelagic organisms are distributed deeper in water which has high rather than low light penetration.

Even though mesopelagic organisms appear to avoid diffuse daylight, there are many reports of artificial light attracting mesopelagic macroplankton and micronekton (e.g. Barham 1966, Lawry 1974, Hirai & Jones 2012). In assessing methods for sampling of mesopelagic fishes, Harrisson (1967, p. 113) pondered 'Why, … , are they not repelled rather than attracted by artificial lights?' In other early experiments, Blaxter & Currie (1967) assessed the effect of artificial lights on mesopelagic acoustic scattering layers in the ocean and basically found repulsion (diving).

Mesopelagic fishes dominate the world total fishes biomass (Irigoien et al. 2014). Recent acoustic abundance estimates (Irigoien et al. 2014) suggest biomass an order of magnitude higher than previous estimates from net catches (Gjøsæter & Kawaguchi 1980). However, the contribution of fish in mesopela-

*Corresponding author: stein.kaartvedt@ibv.uio.no

Publisher: Inter-Research · www.int-res.com

gic SSLs has proved hard to assess for several reasons. First, acoustic backscatter strongly depends on the presence of a swimbladder and its size relative to the acoustic wave length; second, there may be an ontogenetic switch from gas to fat in the swimbladder, corrupting relationships between acoustic and actual sizes; third, mesopelagic fish tend to avoid nets; and fourth, potentially important acoustic targets like fragile siphonophores with gas-filled pneumatophores are poorly sampled (Kloser 2002, Kaartvedt et al. 2012, Davison et al. 2015, Proud et al. 2019).

We aimed at taking advantage of responses to artificial light for assessing the components of mesopelagic SSLs in the Red Sea. We hypothesized that some (unknown) portion of the mesopelagic organisms forming the SSLs would be herded downwards by the light of an remotely operated vehicle (ROV) until trapped and concentrated at the bottom, where they could be identified from ROV video footage. We applied a shipborne echosounder depicting both the ROV and the responding mesopelagic scattering layers while herding the acoustic targets down to an autonomous upward-looking echosounder anchored just above the bottom, the latter providing high-resolution data in deep water. This combined use of acoustics and video enabled concurrent assessment of the response to light at different scales and unveiled a dichotomy including both attraction and repulsion. We evaluate these responses to light applying an individual-based model which reproduced the observed patterns.

2. MATERIALS AND METHODS

2.1. Field work

The study was carried out at a ~700 m deep, nearshore location in the central Red Sea (22.5° N, 39.03° E), the same location as described in Wiebe et al. (2016). We operated a shipborne (the KAUST research vessel RV ‘Thuwal’) echosounder and a rig with upward-looking echosounders located at the bottom (~700 m), in both cases SIMRAD EK60 operated at 38 kHz using transducers with a 7° opening angle. The use of this frequency will bias results towards fish with a swimbladder or other organisms with air inclusions, and most planktonic forms will not be properly detected. Yet 38 kHz is a standard frequency in fisheries research and commonly used in studies of mesopelagic SSLs. The rig was fully autonomous, with a PC built into a pressure-proof container together with acoustic transceivers and powered by batteries in a separate pressure-proof container (system provided by METAS AS). The positively buoyant acoustic rig was anchored with concrete weights. It was deployed on 17 May 2015 and retrieved (acoustic release) on 21 May 2015. The echosounders were pinging every 2 s. Echograms were visualized using Matlab with acoustic values presented as mean volume backscattering strength, S_v (dB re 1 m^{-1}). We operated a SAAB Falcon DR ROV, equipped with 2 LED lights (LED-LAMP-10-Y) (40 W, 2520 lm) and 2 cameras, one HD SUBC imaging 1CAM Alpha 3000 Camera for scientific recording (video and stills) and one vehicle camera for navigation. To make it easier to control the ROV below the ship, a 65 kg iron weight was attached to the ROVs umbilical, around 60 m above the ROV. The ROV was deployed at the location of the bottom-mounted echo sounders on 3 subsequent days (17–19 May). Once at the bottom, the rig was located using a Teledyne Blueview forward looking sonar, model number M900-130-S-STR-MKS. ROVs make noise, with unknown effects on the fauna, so we also tested with the lights turned off.

2.2. Simulation of the herding event

Acoustically observed herding was simulated with an individual-based model, similar to that applied by Dupont et al. (2009) in simulating light-controlled vertical migration. We assumed that individuals of 2 prevailing mesopelagic scattering layers (see Fig. 1) swam randomly within the upper and the lower borders of their so-called light comfort zones (Dupont et al. 2009). The incoming sunlight was set constant, and the light zones therefore corresponded to fixed depth zones, i.e. from ca. 470 to 520 m and from ca. 540 to 630 m depth for the 2 scattering layers, respectively. We simulated 4 different behaviors of the individuals.

In the first case, as the virtual ROV approached the simulated individuals occupying the 2 light comfort zones, individuals responded by directional movement 180° away from the ROV (repulsion) when the distance between the ROV and an individual was less than 50 m and 100 m (±5 SD) of the shallowest and deepest layer, respectively. These maximal repulsion distances were determined according to the observed distances between the ROV and the top of the 2 scattering layers at the time when the first avoidance response was observed in acoustic records.

In the second case, we hypothesized that attraction is facilitated by the light beam of the ROV. Light beams attenuate much more rapidly than diffuse light, and we assumed that the attraction distance, set to 25 m (±5 SD), was shorter than the repulsion distances which presumably were due to diffuse light. The individuals responded by directional movement 180° towards the ROV (attraction) when the distance between the ROV and an individual was less than 25 m (±5 SD), for both layers.

In the third case, individuals responded by both attraction and repulsion as explained above. Thus, in this simulation, individuals closest to the ROV were swimming in the space between the ROV and the maximal attraction distance. Next to this zone, i.e. between the maximal attraction and the maximal repulsion distance, there was a zone where individuals swam away from the ROV. Finally, we also simulated a case with the attraction distance larger (100 and 150 m, ±5 SD) than the repulsion distance (50 and 100 m, ±5 SD).

The simulations were conducted in a virtual water column of 2 dimensions, depth (z, 710 m with dz = 1 m) and width (x, 250 m with dx = 1 m) in addition to time (t, 7200 s with dt = 10 s). This allowed individuals to move both vertically and horizontally over time. We simulated the movement of 20 000 individuals, each with a swimming speed assigned randomly from a normal distribution characterized by a mean swimming speed and an SD. The mean of this distribution was set according to the observed repulsion (i.e. downward) movement of the acoustic layer, 0.11 m s^{-1}, which corresponded to the lowering speed of the ROV. We assumed individual variation that was represented by an SD of 0.03 m s^{-1}. For each simulated time step (10 s), the swimming direction of an individual was set randomly, but constrained by the boundaries of the modelled domain, the natural light comfort zone and by the attraction and repulsion zones of the ROV as defined above. Within the attraction/repulsion zones of the ROV, individuals swim towards/away from the ROV.

The results of the simulation are presented similar to that of echograms, i.e. the logarithmic ($\log_{10}$) depth-dependent density of individuals was calculated by integration of the individuals every time step (10 s) and for each depth bin (1 m) inside the acoustic beam with an angle of 7 degrees, and then graded according to a color scale. The horizontal width of the ship-based acoustic beam is between 49 and 73 m between a depth of 400 and 600 m, and the width of the model domain was set sufficiently wide (250 m) to avoid boundary effects when integrating.

3. RESULTS

3.1. Acoustics and ROV

In undisturbed conditions, 2 vertically migrating mesopelagic scattering layers were particularly conspicuous (Fig. 1A). One layer had daytime distribution reaching >600 m and one had its core from ~450 to 500 m. Organisms from these layers ascended into the upper 100–200 m at night (Fig. 1A).

No herding was apparent with the lights of the ROV turned off (not shown). On the other hand, basically all acoustic targets forming these scattering layers were herded downwards in the experiment with the lights of the ROV turned on, leaving voids in the backscatter at the previous depths of the SSLs (Figs. 1B,C). Both the ROV and the SSLs were visible in the echogram from the shipborne echosounder (Fig. 1B), and it appeared that organisms of both SSLs mostly were diving in front of the descending vehicle. Nevertheless, the echogram also indicates abundant acoustic targets just above the ROV (Fig. 1B).

The first diving responses started with the ROV at ranges ~50 and 100 m above the 2 SSLs, respectively. The nearly universal response to the ROV, with little backscatter remaining in the water column as the targets were herded downwards, was particularly evident in results from the bottom-mounted echosounder (Fig. 1C), which was closer to the acoustic targets and hence gives the better resolution. Note that since the acoustic beam becomes progressively narrower with declining distance from the echosounder and that the lowermost meters towards the bottom were not covered the number of targets will decrease close to this echosounder.

The high-resolution data from the deployed echosounder provided many successive echoes from the same individual and showed that some targets initially affected by the ROV subsequently ascended towards their original vertical distribution, reforming SSLs (Fig. 1C). Results from the vessel-mounted echosounder show how other targets were herded into waters below the autonomous echosounder, i.e. avoiding the descending ROV (Fig. 1B), eventually largely merging with the bottom echo.

The echograms showed that the scattering layers largely, though not exclusively, were herded downwards in front of the ROV, while the video footage documented concurrent abundant concentrations of fish swarming in its lights (Fig. 2A, Video S1 in the Supplement at www.int-res.com/articles/suppl/m625p225_supp/). Footage of the former mesopelagic

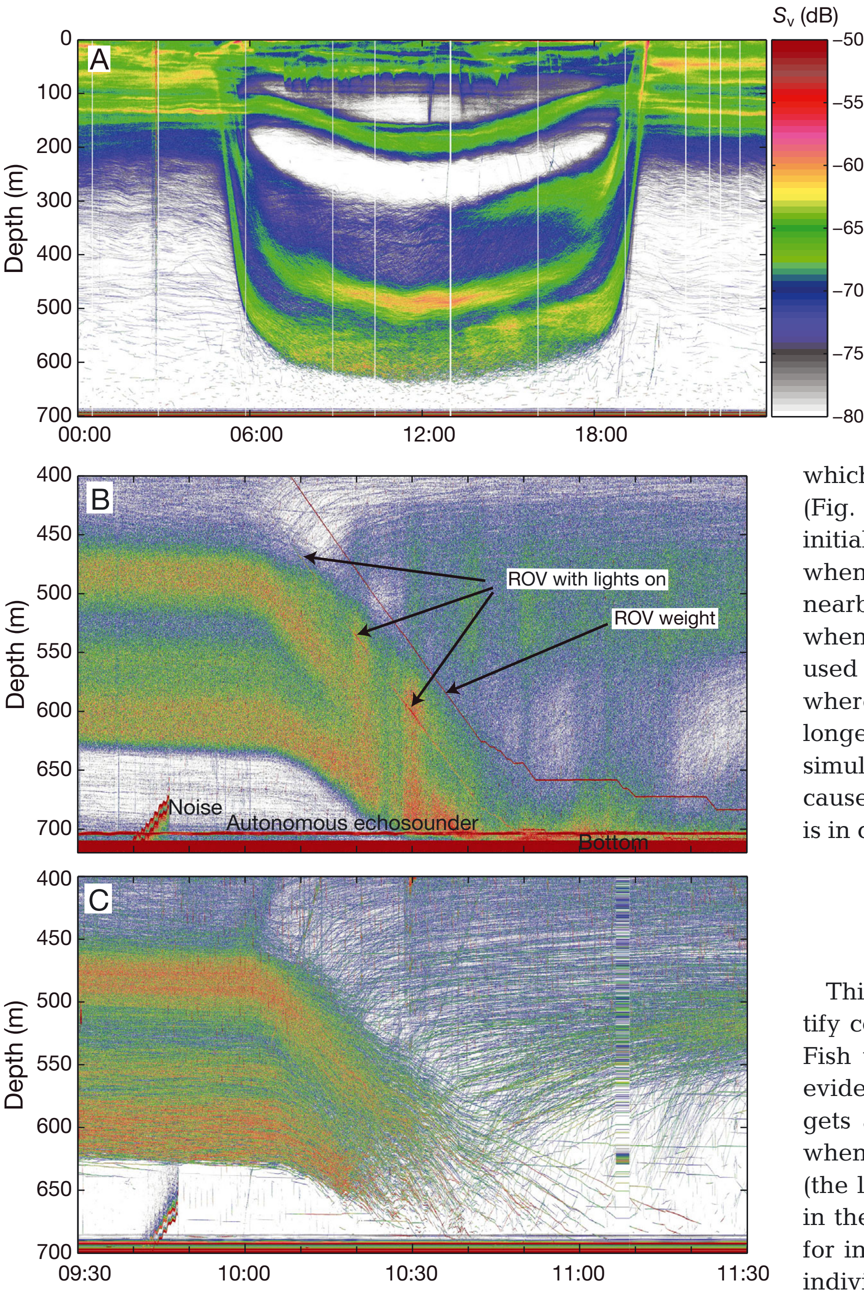

Fig. 1. (A) Diel echogram (20 May 2015). (B,C) Manipulating the vertical distribution of mesopelagic scattering layers using a remotely operated vehicle (ROV) with artificial light. (B) Echogram (38 kHz) from the ship operating the ROV (depicted in the echogram). (C) Simultaneous echogram (38 kHz) from an upward-looking autonomous echosounder located at the bottom. Color scale refers to volume backscatter (S_v), a proxy for abundance

acoustic targets, now trapped at the bottom, only revealed fish (Fig. 2B, Video S1). Hence, the targets pushed downwards in front of the ROV were fish, as were the ones attracted to and swarming in the lights of the ROV.

3.2. Modeling

In the initial simulation, individuals were assigned repulsion distances of 50 and 100 m for the shallowest and the deepest layer, respectively (Fig. 3A). This simulation reproduced the very first downward movement of the 2 layers apparent in the observed echogram at around 10:00 h (Fig. 1B,C). However, in addition to repulsion, seen as downward movement away from the ROV, the observed echogram also indicates acoustic targets above the ROV, which appear to follow the ROV downwards (Fig. 1B). This pattern is not recognized in the initial simulation (Fig. 3A), but is reproduced when the simulated individuals are assigned a nearby (25 m) attraction zone (Fig. 3B), and also when both repulsion and attraction zones are used simultaneously (Fig. 3C). In the case where the attraction distance was assumed longer than the repulsion distance (Fig. 3D), the simulation shows an initial upward movement caused by a distant attraction to the ROV, which is in contrast to the acoustic observations.

4. DISCUSSION

This study provides a novel approach to identify components of mesopelagic acoustic SSLs. Fish were the dominant targets at 38 kHz as evidenced by the direct observations of the targets and by moving entire mesopelagic SSLs when fish were herded down to the bottom by (the light of) the ROV. There was a dichotomy in the fishes' response to the descending ROV for individuals in both scattering layers. Some individuals evidently were attracted to and accumulated in the light of the vehicle, while the acoustic records showed that avoidance of the ROV in fact was the main response. However, regardless of individuals being 'pulled' (see also Dypvik & Kaartvedt 2013) or 'pushed' downwards, the targets forming the SSLs were the same as those herded downwards by the ROV and those being visually observed swarming in its light and accumulating at the bottom. In essence, fish form the mesopelagic SSLs at 38 kHz in the Red Sea.

Few mesopelagic fish species prevail in the Red Sea (Dalpadado & Gjøsæter 1987), and *Benthosema*

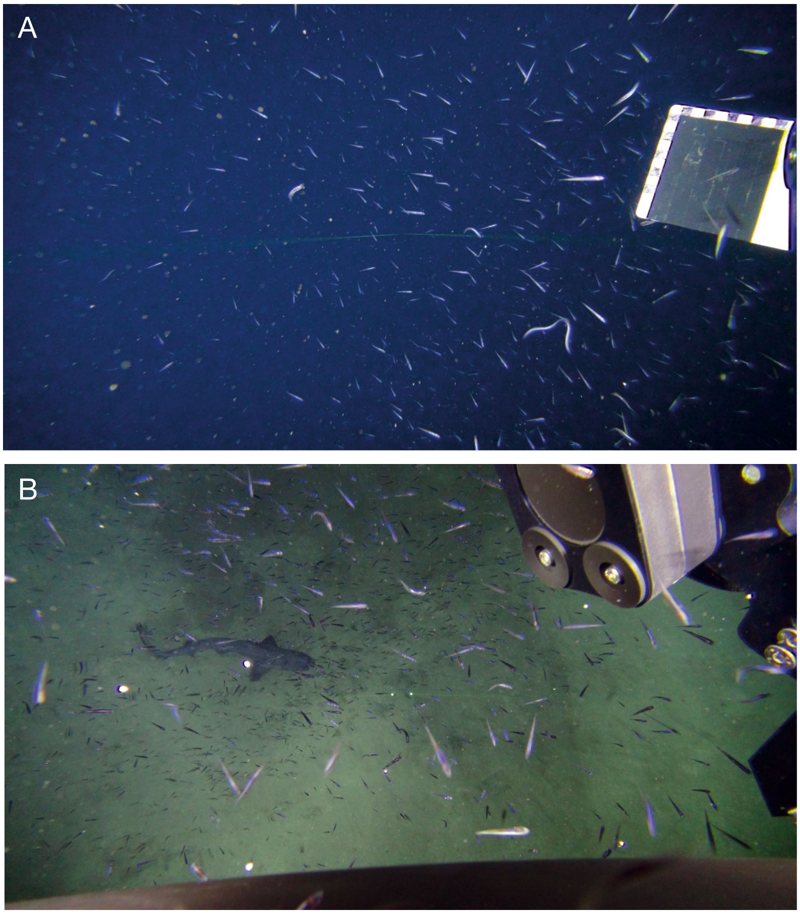

Fig. 2. Photos from the remotely operated vehicle (ROV) camera. (A) Fish swarming in the light of the ROV. (B) Fish that have been herded to the bottom. A shark in apparent feeding frenzy (tentatively idenfied as *Lago omanensis*) is exploiting the high concentration of prey in the light of the ROV (see Video S1 in the Supplement)

pterotum is the predominant fish in catches from the lower layer and *Vinciguerria* in the layer above (Dypvik & Kaartvedt 2013, S. Kaartvedt unpubl. results). The visual observations were in accordance with such findings, although we could not make proper species identifications from the images. In addition, a few barracudinas (likely *Lestrolepis* sp.) appeared in the video footage.

It is well known that mesopelagic fish may be attracted to artificial light (Barham 1966), including species in the Red Sea (Dypvik & Kaartvedt 2013). As noted by Harrisson (1967), this is a paradox since their normal behavior is to avoid light. The contradicting responses observed here may add to this enigma, though the simulations provide a potential explanation in distinguishing between responses to diffuse light and point sources. It might be that oceanic twilight organisms have adapted differently in response to point light sources such as bioluminescence than to diffuse light from above (Warrant & Locket 2004). If the behavioral response to such natural point sources is attraction, we speculate that not too distant artificial light, seen as a point source, triggers attraction. On the other hand, when the artificial light is more distant and perceived as diffuse light, the response is repulsion, as in the case of sunlight.

From these arguments it can be hypothesized that the attraction distance to an artificial light beam is proportional to the length scale given by the reciprocal beam attenuation coefficient, c (m^{-1}), while the repulsion distance is proportional to the reciprocal attenuation coefficient for diffuse light, K (m^{-1}). Since a beam (parallel straight lines) is attenuated by both absorption and scattering, while downwelling irradiance in the ocean is only partly attenuated by scattering in addition to absorption (Kirk 2011), c is always larger than K. Therefore, the attraction distance is likely to be shorter than the repulsion distance as also indicated in our simulation results, where the inverse assumption (attraction distance > repulsion distance) yielded unreasonable predictions (Fig. 3D).

From the observed echogram (Fig. 1B) it can be seen that the shallowest and the deepest layer are repulsed approximately at the same time (around 10:15 h) by the ROV. This suggests that the organisms of the shallowest layer have shorter repulsion distance than those of the deepest layer. This is expected since the ambient natural irradiance of the organisms of the shallowest layer is higher than the ambient light of those in the deepest layer. Thus, in order for the ambient artificial light of the organisms to be equally strong or stronger than the natural ambient irradiance, the ROV needs to be closer to the shallowest than the deepest scattering layer. We believe the above hypothesis is useful for future experimentation.

The experimental approach used in this study requires a relatively shallow location, facilitating herding to the bottom, yet it would be applicable e.g. at continental margins and sea mounts (cf. O'Driscoll et

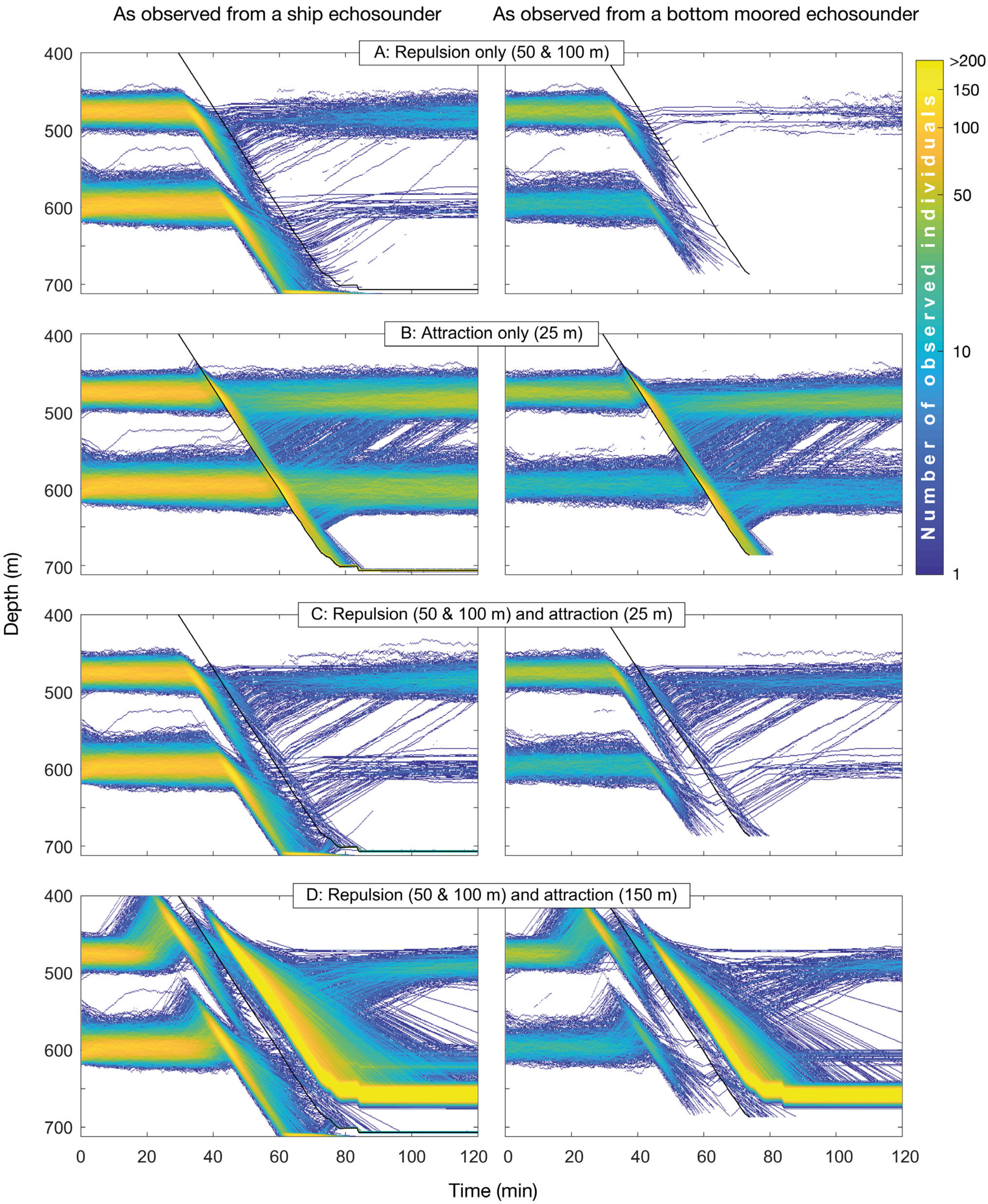

Fig. 3. Simulation of herding events as observed from ship-mounted (left) and bottom-mounted echosounders (right) using an individual based model (simulation of 20 000 individuals). Results for repulsion only (A), attraction only (B), both attraction and repulsion (C) and attraction and repulsion with the attraction distance longer than the repulsion distance (D). Color scale refers to the logarithmic ($\log_{10}$) depth dependent density of individuals

al. 2012). The organisms forming the mesopelagic SSLs in the Red Sea display unusual universal and regular DVM behavior (i.e. responses to light; cf. Fig. 1A; Dypvik & Kaartvedt 2013) compared to other oceans (Klevjer et al. 2016). More diverse responses to corresponding experiments would be expected elsewhere and with inclusion of additional acoustic frequencies. Resolution of individual acoustic targets at different frequencies would allow establishing *in situ* acoustic target strengths and therefore acoustic abundance estimates of different size classes. Concurrent observations at different scales enabled us to document both attraction and repulsion to the light source. We applied white light, yet the organisms at depth are adapted to much narrower wave lengths (Warrant & Locket 2004). Experiments including varying light quantities and qualities would be a natural next step in studying organisms of the twilight zone.

Acknowledgements. The study was funded by King Abdullah University of Science and Technology (KAUST). We thank Francis Luke Mallon and Brian C. Hession for skillful operation of the ROV and the crew of RV 'Thuwal' for help during the cruise.

LITERATURE CITED

Aksnes DL, Røstad A, Kaartvedt S, Martinez U, Duarte CM, Irigoien X (2017) Light penetration structures the acoustic scattering layers in the global ocean. Sci Adv 3: e1602468

Barham EG (1966) Deep scattering layer migration and composition: observations from a diving saucer. Science 151: 1399–1403

Bianchi D, Galbraith ED, Carozza DA, Mislan KAS, Stock CA (2013) Intensification of open-ocean oxygen depletion by vertically migrating animals. Nat Geosci 6: 545–548

Blaxter J, Currie R (1967) The effect of artificial lights on acoustic scattering layers in the ocean. Symposia of the Zoological Society of London, London, p 1–14

Dalpadado P, Gjøsæter J (1987) Observations on mesopelagic fish from the Red Sea. Mar Biol 96:173–183

Davison PC, Checkley DM Jr, Koslow JA, Barlow J (2013) Carbon export mediated by mesopelagic fishes in the northeast Pacific Ocean. Prog Oceanogr 116:14–30

Davison PC, Koslow JA, Kloser RJ (2015) Acoustic biomass estimation of mesopelagic fish: backscattering from individuals, populations, and communities. ICES J Mar Sci 72:1413–1424

Dupont N, Klevjer TA, Kaartvedt S, Aksnes DL (2009) Diel vertical migration of the deep-water jellyfish *Periphylla periphylla* simulated as individual responses to absolute light intensity. Limnol Oceanogr 54:1765–1775

Dypvik E, Kaartvedt S (2013) Vertical migration and diel feeding periodicity of the skinnycheek lanternfish (*Benthosema pterotum*) in the Red Sea. Deep Sea Res I 72: 9–16

Gjøsæter J, Kawaguchi KA (1980) A review of the world resources of mesopelagic fish. FAO Fish Tech Pap 193: 1–151

Harrisson CMH (1967) On methods for sampling mesopelagic fishes. Symp Zool Soc Lond 19:71–126

Hirai J, Jones DOB (2012) The temporal and spatial distribution of krill (*Meganyctiphanes norvegica*) at the deep seabed of the Faroe–Shetland Channel, UK: a potential mechanism for rapid carbon flux to deep sea communities. Mar Biol Res 8:48–60

Irigoien X, Klevjer TA, Røstad A, Martinez U and others (2014) Large mesopelagic fishes biomass and trophic efficiency in the open ocean. Nat Commun 5:3271

Kaartvedt S, Staby A, Aksnes DL (2012) Efficient trawl avoidance by mesopelagic fishes causes large underestimation of their biomass. Mar Ecol Prog Ser 456:1–6

Kaartvedt S, Langbehn TJ, Aksnes DL (2019) Enlightening the oceans' twilight zone. ICES J Mar Sci 76:803–812

Kampa EM (1971) Photoenvironment and sonic scattering. In: Farquhar B (ed) Proceedings of an International Symposium on Biological Sound Scattering in the Ocean Maury Center for Ocean Science. US Government Printing Office, Washington, DC, p 51–59

Kirk JTO (2011) Light and photosynthesis in aquatic ecosystems. Cambridge University Press, Cambridge

Klevjer TA, Irigoien X, Røstad A, Fraile-Nuez E, Benítez-Barrios VM, Kaartvedt S (2016) Large scale patterns in vertical distribution and behaviour of mesopelagic scattering layers. Sci Rep 6:19873

Kloser RJ (2002) Species identification in deep water using multiple acoustic frequencies. Can J Fish Aquat Sci 59: 1065–1077

Lawry JV (1974) Lantern fish compare downwelling light and bioluminescence. Nature 247:155–157

O'Driscoll RL, de Joux P, Nelson R, Macaulay GJ and others (2012) Species identification in seamount fish aggregations using moored underwater video. ICES J Mar Sci 69: 648–659

Proud R, Handegard NO, Kloser RJ, Cox MJ, Brierley AS (2019) From siphonophores to deep scattering layers: uncertainty ranges for the estimation of global mesopelagic fish biomass. ICES J Mar Sci 76:718–733

Warrant EJ, Locket NA (2004) Vision in the deep sea. Biol Rev Camb Philos Soc 79:671–712

Wiebe PH, Bucklin A, Kaartvedt S, Røstad A, Blanco-Bersial L (2016) Vertical distribution and migration of euphausiid species in the Red Sea. J Plankton Res 38: 888–903

Editorial responsibility: Franz Mueter, Juneau, Alaska, USA

Submitted: April 29, 2019; Accepted: July 19, 2019
Proofs received from author(s): August 16, 2019